energies

MDPI

Article

Optimal Sizing of a Real Remote Japanese Microgrid with Sea Water Electrolysis Plant Under Time-Based Demand Response Programs

Mahmoud M. Gamil [1,*], Makoto Sugimura [1], Akito Nakadomari [1], Tomonobu Senjyu [1,*], Harun Or Rashid Howlader [1], Hiroshi Takahashi [2] and Ashraf M. Hemeida [3]

1 Department of Electrical and Electronics Engineering, Faculty of engineering, University of The Ryukyus, 1 Senbaru, Nishihara-cho, Nakagami, Okinawa 903-0213, Japan; e155528g@gmail.com(M.S.); akito.nakadomari@gmail.com (A.N.); h.h.howlader@ieee.org (H.O.R.H.)
2 Fuji Elctric Co., Ltd, Tokyo 141-0032, Japan; takahashi-hirosi@fujielectric.com
3 Department of Electrical Engineering, Faculty of Energy Engineering, Aswan University, Aswan 81528, Egypt; ashraf@aswu.edu.eg
* Correspondence: f195a036@cs.u-ryukyu.ac.jp (M.M.G.); b985542@tec.u-ryukyu.ac.jp (T.S.)

Received: 25 May 2020; Accepted: 11 July 2020; Published: 16 July 2020

Abstract: Optimal sizing of power systems has a tremendous effective role in reducing the total system cost by preventing unneeded investment in installing unnecessary generating units. This paper presents an optimal sizing and planning strategy for a completely hybrid renewable energy power system in a remote Japanese island, which is composed of photovoltaic (PV), wind generators (WG), battery energy storage system (BESS), fuel cell (FC), seawater electrolysis plant, and hydrogen tank. Demand response programs are applied to overcome the performance variance of renewable energy systems (RESs) as they offer an efficient solution for many problems such as generation cost, high demand peak to average ratios, and assist grid reliability during peak load periods. Real-Time Pricing (RTP), which is deployed in this work, is one of the main price-based demand response groups used to regulate electricity consumption of consumers. Four case studies are considered to confirm the robustness and effectiveness of the proposed schemes. Mixed-Integer Linear Programming (MILP) is utilized to optimize the size of the system's components to decrease the total system cost and maximize the profits at the same time.

Keywords: microgrid; RTP; demand response; sea water electrolysis plant; MILP; optimal sizing; minimum cost; renewable energy power system

1. Introduction

Emissions of greenhouse gases (GHGs) are increasing every day, and the awful impacts of GHGs are often regarded as one of the greatest dangers to the world's biological framework and human race [1]. In 2014, the worldwide carbon emissions were amounted to over 36 billion tons, which is approximately 1.6 times the 1990s rates [2]. Over the past few decades, a significant increment in the global average temperature is experienced as a result of GHGs and it is expected to increase. These environmental changes threaten human health and the economy of various nations around the earth [3]. According to the Kyoto Protocol in 1997, general commitments were considered by all members, and four greenhouse gases (GHGs) were identified to be significantly reduced by 37 of the highly industrialized countries. Many nations around the world are getting ready to diminish their CO_2 discharges to avert the most extremely terrible outcomes of the environmental changes.

Japan is focused on decreasing CO_2 emanations, and the Prime Minister Hatoyama vowed in 2010 that his nation would lower CO_2 discharges by 25% in 2020 compared to the levels in the 1990s [4].

The gross CO_2 emissions in Japan were 1241 Mt in 2011, where 37.1 percent of this amount originated from the energy sectors, and 27.3 percent came from the industrial sectors. In order to avert the potential threats of GHGs, changing to sustainable power sources is viewed as the most appropriate approach to make an incredible decrease in GHG emissions [5]. The objective of decreasing half of GHG outflows by 2050 has been considered as a concrete objective to moderate the earth's temperature increase [6]. The internationally supported change to a low-carbon resilience model coordinates higher portions of renewable energy, especially in power system planning [7].

Sustainable power sources are increasingly becoming more viable everywhere throughout the world and have an immense potential to fulfill future power requirements [8]. As indicated by the insights of the International Renewable Energy Agency (IRENA), the portion of renewables in electricity generation will ascend from 25% today to 86% in 2050. Approximately 60% of all produced electricity in 2050 will be contributed by renewables like power from sunlight and wind. The yearly inexhaustible power production would ascend from 7000 TWh at present to 47000 TWh by 2050. The introduction of variable renewable energies such as wind and PV (photovoltaics) in a country's energy blend has been in the spotlight for socio-environmental conservation issues to tackle energy security problems [9], especially after the Great East Japan Earthquake and the Fukushima atomic mishap in Japan. A 100% sustainable power source network in Japan by 2030 is demonstrated to have the option to accomplish an elevated level of power efficiency [10,11].

As renewable energy sources are relying upon climate conditions, hybrid energy storage systems (ESSs) are used to store surplus power to supply power to loads in case of low solar radiation or low wind speed. Batteries are one of the most appealing storage systems due to their high efficiency and low environmental pollution effects [12,13]. The only problem of BESS is its high installation cost, so it is essential to ensure optimal sizing to maximize the profit of renewable energy systems and encourage its marketization. In microgrids, not only the excess power can be stored in BESS for future uses when the generated power is lower than the load requirements, but BESS is also used to protect microgrids from instabilities from load changes or outage of connected generating units [14,15].

As a result of the lack of petrochemical resources and their unsustainable behavior, fuel cells have grabbed more attention because of their high efficiency and their environmental friendliness. A fuel cell is an electrochemical tool that converts chemical energy into electrical power directly with high efficiency [16]. Fuel cells are desirable than other traditional energy storage systems for both on-site activities of energy production and mobile purposes due to efficient recharging and longer running times [17]. Hydrogen storage is a technical barrier to the growth of the fuel cell industry. Hydrogen can be preserved as a high pressure compressed gas, liquefied fluid, or kept by combining with other materials [18]. There are two kinds of fuel cell systems: Discrete FC (DFC) and Unitized FC (UFC). Instead of combining all functions in a single device into a UFC, the electrolysis cycle and power generation are separated into two devices in a DFC network [19].

Smart grid these days utilizes hydrogen storage technologies. When electricity price is low, electrolyzers use energy for hydrogen production to be stored in tanks. As electricity prices rise, fuel cells will generate electricity from the accumulated hydrogen [20]. Chemical substances are produced in the system during the electrolysis process, which can gain revenues to pay back some parts of the total system cost. Sodium hypochlorite (NaClO) is one of the vital chemical products of the seawater electrolyzing process. It is used for surface and material cleaning, bleaching, disinfectant, eliminating smells, drinking water disinfection, and removing stains from clothing. It has many benefits such as easy handling, secure storage, safe transportation, etc. Most bacteria and viruses are affected by its household bleach, and microorganisms can not develop any protection against it [21].

Off-grid power system usually suffers from low load factor, which increases the required number of batteries to meet the load demand and causes a consequent increase in the total system cost. One of the verified options to solve this problem is to apply suitable demand response strategies [22]. Demand Response (DR) programs can give a lower cost option in contrast with spinning reserves and faster response than other generation control to maintain system stability. By applying demand

response programs, the number of generating units will be less as demand is distributed over all periods of day's hours [23]. Demand response includes accomplishing changes in power requests at different times—for instance, moving demand from top to off-top demand periods. This can be done by means of price signals, monitoring of equipment, and direct control of individual loads [24]. Demand response is definitely not a new concept, yet it plays a great role in most countries to guarantee system power balance constraints. Typically, the DR programs are organized into one of two categories: Incentive-Based Program (IBP) and Time-Based Program (TBR) systems. Time-based programs include Time of Use (TOU), RTP, Critical Peak Pricing (CPP), and so on. Incentive-based programs include Direct Load Control (DLC), Emergency Demand Response Program (EDRP), Interruptible load (IL), Capacity market Program (CAP), etc. [25].

Many authors have studied the optimum operation of hybrid microgrids, including demand response and renewable energy. In [26], the authors used Genetic Algorithms (GAs) with multi-objectives, which are integrated in HOMER software for optimal sizing of hybrid renewable systems with wind and solar energy generators and compared the results with HYRES tool in MATLAB. The optimal integration of renewable energy conversion systems, including PV and wind generators in microgrid with reversible solid oxide cells (rSOC), is presented in [27]. The Improved Hybrid Optimization using Genetic Algorithm (iHOGA) is used for optimal sizing of a hybrid renewable energy system in [28], taking into consideration different values of loads and various acquisition costs of HRES. Shunichi Fukuzum et al. focused their research on the production of fuel from seawater and its direct use in fuel cells, as it is the most abundant resource of fuel in our planet [29]. In PV power integrated microgrids, hydrogen produced by seawater electrolysis can be used in FC to generate electricity at night [30]. According to the authors of [31], three separate hypothetical hydrogen-producing plants were studied for hydrogen storage in a compressed state. Moreover, the results showed that low-temperature electrolysis technologies are the best available option at this moment. In [32], the authors intended to investigate the variation of the tension and energy consumption at electrolysis of natural seawater comparative with electrolysis of a solution of 15% NaOH, in the same conditions.

RTP, which is deployed in this research work, is briefly discussed in [33]. In RTP, electricity tariffs change over time which mirrors the genuine market cost. RTP is enabled by using advanced meters and automatic energy consumption planning tools, which helps consumers to get cheap electricity and makes the power system more reliable [34].

For this study, the microgrid under study is located on the island of Okinawa. Okinawa Prefecture is an isolated touristic island located in the Pacific Ocean and the Eastern China Sea in the south of Japan. The annual number of visiting tourists is over than 7.16 million and continues to grow. More than 80% of its energy needs depends on thermal power, especially coal-fired power stations [35]. Okinawa's energy policy goals are to minimize reliance on fossil fuels, diversify energy sources, and increase the energy self-sufficiency rate, so it has already taken measures to establish large-scale mega-solar generation facilities, encourage micro-grids, electric cars, biofuels, natural gas usage, and judicious use of excess energy. Therefore, the main contribution of the proposed scheme in this manuscript in view of all the above are as follows.

1. An optimal sizing approach of a real remote Japanese island using renewable energy sources is proposed.
2. Demand response methodology is considered with a complete study for its effects on the optimal sizing schemes.
3. The seawater electrolysis plant is implemented to deepen the idea of effective investment in power system facilities.
4. Four case studies with detailed analysis are considered to confirm the robustness and effectiveness of the proposed scheme.

The frame of the remaining sections of this paper is written as follows, in Section 2, the system is described, while the demand response program is discussed in Section 3, especially the adopted (RTP) type. In Section 4, the system constraints and the objective function are introduced using MILP optimization technique. Different scenarios are simulated and discussed in Section 5; the comparison between four optimized systems is discussed in Section 6. Conclusion and future work are then presented in Section 7.

2. System

The power system model of this research is shown in Figure 1, whereas the operation of the system is illustrated in the flow chart of Figure 2. In typical operation, the load demand is met from PV and WG. If there is surplus power, it is used to charge the BESS, and if there is other excess power, it will be used by electrolysis plants to produce hydrogen (H_2) for fuel cell usage. In the case of power shortage, load power demand is supplied by BESS. FC will be used if BESS is not sufficient to meet the excess load power. Demand response programs are applied to increase the system efficiency and decrease the loss of load probability. The most crucial issue is to reach minimum system cost, taking into consideration the system constraint. In this paper, MILP is used in sizing the system to reach the optimal cost schemes taking into consideration the revenue from chemical products of the electrolysis process. The system components are discussed in the following sections.

2.1. FC

Fuel cells (FCs) are electrochemical systems that produce DC electricity by mixing hydrogen with oxygen. Fuel cells comprise two terminals (anode and cathode) and an electrolyte. The following equations demonstrate the chemical reactions inside it [36].

$$H_2 \longrightarrow 2H^+ + 2e^- \tag{1}$$

$$0.5O_2 + 2e^- \longrightarrow O^{2-} \tag{2}$$

$$2H^+ + \frac{1}{2}O_2^{2-} \longrightarrow H_2O + heat \tag{3}$$

It is necessary to connect several fuel cells in series because of the minimum voltage produced from single cell. It is also needed to install a DC–DC boost converter to increase the voltage and heal the voltage variation from no-load to full-load conditions, which can reach 50%. The following equations show the electrical voltage and power equations of the fuel cell [36],

$$V_{FC} = E - V_{act} - V_{con} - V_{ohm} \tag{4}$$

$$E = n_{cel}\left(1.229 - 0.85 \times 10^3 (T - 298.15) + \frac{RT}{2F} ln\left(\frac{P_{H_2}.\left(P_{O_2}\right)^{1/2}}{P_{H_2O}}\right)\right) \tag{5}$$

where V_{FC} is the output voltage of fuel cell; E is the internal voltage; V_{act} is the activation voltage; V_{ohm} is ohmic losses; V_{con} is the concentration losses; P_{H_2}, P_{O_2}, and P_{H_2O} are the partial voltages of hydrogen, oxygen, and water (atm/kmol), respectively; R the is the universal gas constant; T is the temperature in (^{0}K); F is the Faraday constant; and n_{cel} is the number of cells linked in series.

$$V_{act} = \frac{RT}{\alpha nF} ln\left(\frac{I_{FC}}{j_o.S}\right) \tag{6}$$

$$V_{con} = \frac{RT}{nF} ln\left(1 - \frac{I_{FC}}{i_1}\right) \tag{7}$$

$$V_{ohm} = R * I_{FC} \tag{8}$$

$$I_{FC} = n.F.Uf.M_{comb} \tag{9}$$

$$P_{FC} = V_{FC} * I_{FC} \tag{10}$$

$$P_{FC} = V_{FC} * I_{FC} \tag{11}$$

where R is the ohmic resistance, n is the number of electrons exchange, Uf is fuel utilization, M_{comb} is mass flow, and P_{FC} is the output power of FC.

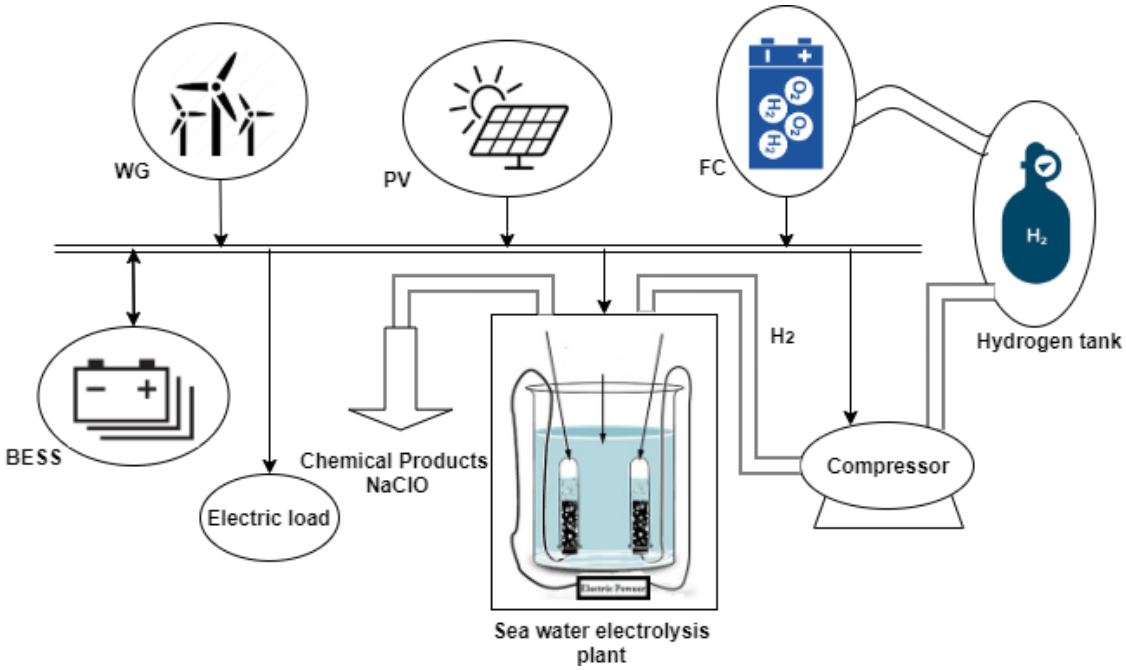

Figure 1. Proposed power system.

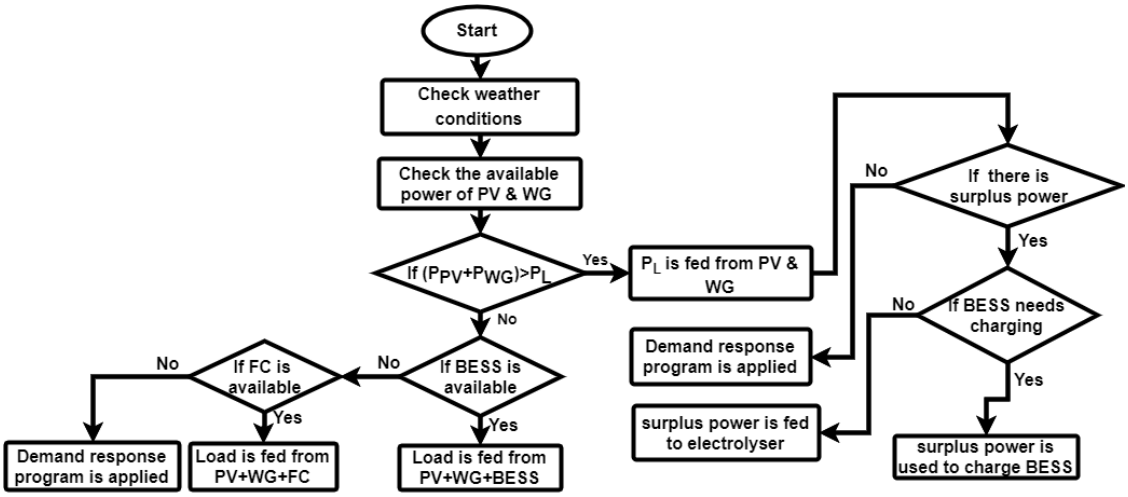

Figure 2. The flow chart of the system ordinary mechanism.

For distributed generation (DG) applications, solid oxide fuel cells (SOFC), polymer electrolyte membrane fuel cells (PEMFC), and molten carbonate fuel cells (MCFC) are probably preferred to be utilized. Fuel celled distributed generation systems have several merits like high efficiency, zero outflow of harmful emissions, and easy to install at any location in a power system for network support [37].

2.2. PV

Solar power is converted to electricity by transferring the falling solar irradiation on the surface of Photovoltaic cells to electric energy [38]. The arrangement of several series/parallel PV cells results in a photovoltaic system with a nonlinear current–voltage (I–V) characteristic depending on the level of irradiation and the cell temperature. Equation (12) shows the power of PV as a function of solar radiation and temperature [39]:

$$P_{PV} = P_{PVRated} * DF_{PV} \left(\frac{E_t}{E_{t,STC}} \right) * [1 + \alpha_{temp}(T_{cell} - T_{cell,STC})] \quad (12)$$

where P_{PV} is the output power of the PV array (kW), $P_{PVRated}$ is the rated capacity of the PV array at STC (kW), DF_{PV} is the PV derating factor (%), E_t is the total global irradiance incident on the PV array (kW/m^2), $E_{t,STC}$ is the solar irradiation incident at STC (1 kW/m^2), α_{temp} is the temperature coefficient of power, T_{cell} is the PV cell temperature at the current time step (^0c), and $T_{cell,STC}$ is the PV cell temperature at STC (25 °C).

Optimal PV power plant sizing is essential in the establishment process to reduce the cost and the number of the required system's components. Furthermore, optimum inverter selection for ideal PV power plant relies upon its characteristics and varies from kilowatts to over than one megawatt. This matter inspires engineers to develop new technologies to solve the problem of the PV plants sizing. Japan is the third-largest PV capacity in the world; PV also has a considerable impact on its national power system [40,41].

2.3. WG

Wind energy is converted to electricity by means of wind turbine combined electrical generators. Wind power is affected by wind speed and the turbine hub height. Therefore, to bypass any expected error, the wind speed ought to be accurately estimated at the hub of the turbine. Wind speed can be translated to wind power by using Equation (13) [42]:

$$P_W = \frac{1}{2} C_P A \rho_{air} v^3 \quad (13)$$

where P_w is the power output of the turbine, C_p is the turbine power coefficient, A is the swept area of the turbine (m^2), ρ_{air} is the air density (kg/ m^3), and v is the wind speed (m/s). C_p and ρ_{air} are not constant and vary widely over weather conditions.

The wind power system consists of a large number of small generators, connected by a particular voltage network. The positioning of wind turbines for each location needs to be well studied to evaluate the turbine load and where the turbine performs better [43].

2.4. BESS

The battery energy storage system (BESS) can offer versatile energy management options that can boost power systems' performance efficiency. The battery system comprises at least one electrochemical cell, and cells are arranged in series or parallel. Through an electrochemical reaction, the stored energy is transformed into electrical energy [44]. The proper sizing of the BESS is an essential issue in micro-grids to reduce overall cost. The State Of Charge (SOC) is one of the main parameters of batteries; it is characterized as the proportion of its current capacity$(Q(t))$ to the nominal limit (Q_n). The nominal capacity describes the greatest measure of the charge that can be put away in the battery [45]. The following equation can define the SOC.

$$SOC(t) = \frac{Q(t)}{Q_n} \quad (14)$$

Estimating *SOC* is a basic battery use problem. It defines its remaining power and reflects the battery effectiveness. It also helps to secure battery, avoid over-discharging, and increase battery lifetime, so it is essential to take *SOC* value into consideration within control constraints to keep it within specific limits (20% and 80% for most control strategies).

2.5. Sea Water Electrolysis

Approximately 75% of our planet's surface is covered with water. Sadly, the majority of this water is saline water. However, that vast amount of water can be used for hydrogen production instead of using pure water [46]. Equations (15)–(18) represent the chemical equations during the electrolyzing process [26,47]:

$$NaCl + H_2O \longrightarrow NaClO + H_2 \tag{15}$$

$$2Na^+ + 2H_2O + 2e^- \longrightarrow 2NaOH + H_2 \tag{16}$$

$$2NaOH + Cl_2 \longrightarrow 2NaClO + H_2 \tag{17}$$

The overall equation during the electrolysis process:

$$NaCl + H_2O \longrightarrow NaClO + H_2 \tag{18}$$

Compressed gas storage is the easiest way for hydrogen storage. It needs only a compressor and a pressure vessel. The only barrier of this method is the immense cost for high storage pressures' capacities [48].

The inlet, outlet pressures, and flow rate are the parameters that set the required power of the compressor and specify its cost. Both centrifugal and reciprocating compressors can be used in hydrogen applications. Although centrifugal compressors have lower efficiency, they are 50% cheaper than reciprocating ones. The compressor cost is calculated through the following equations,

$$cost_{comp} = 4000 * 1000 * \left(\frac{P_{comp}}{4000}\right)^{0.8} * \left(\frac{PR_f}{20}\right)^{0.18} \tag{19}$$

$$P_{comp} = Q_{H2} * 2.2 * \frac{ln\,(PR_F/0.1)}{ln\,(20/0.1)} \tag{20}$$

$$Cost_{tank} = 1323 * 227 * \left(\frac{Q_{H2} * 24 * N * 20}{227 * PR_F}\right)^{0.75} * \left(\frac{P_F}{20}\right)^{0.44} \tag{21}$$

where PR_f is the final outlet pressure, P_{comp} is the power of compressor [kW], Q_{H2} is the flow rate [kg/h] of hydrogen, and N is the storage time (taken as 7 days).

3. Demand Response

DR programs help in shaping the load demand curve and distributing the peak load demands to lower demand periods. DR provides several benefits not only to power system operation, but also for consumers. Their main merits are described as below.

1. It supports reducing the electricity cost and avoids wasteful investments in networks for generation, transmission, and distribution.
2. It decreases the electric demand during the contingencies of the power system, so it enhances reliability, increases power system security, ameliorates the stress condition of the system, and prevents load shedding occurrences.
3. It aids greater integration of renewable energy resources in electrical power systems, as DR systems help to overcome the uncertainty of sustainable energy, which leads to efficiency improvement.

4. Consumers benefit from bill reduction via the use of DR services by rearranging their consumption [49].

Real-Time Pricing (RTP)

By applying RTP programs, the price of electricity regularly varies with wholesale market rates. Dynamic electricity price signals are always available to the consumers one hour or one day in advance. These signals help utility companies efficiently to manage electricity prices to represent demand-driven elastics and inspire consumers to regulate their electricity consumption to get monetary advantages.

Smart meter infrastructures are the most crucial issue in RTP implementation. Energy elastics application is emerged with smart meters for informing real-time prices to consumers and tracking electricity consumption according to informed prices [50].

In this work, the model for user response to electricity price is modeled by Equations (22)–(24) [51]. As the price increases or decreases, the electric load demand responds by increasing or decreasing,

$$lvr(t) = a.exp(-ep(t)/b) + c \tag{22}$$

$$\Delta P_L(t) = lvr(t).P_L(t) \tag{23}$$

$$P_{LRTP}(t) = P_L(t) + \Delta P_L(t) \tag{24}$$

where lvr is the variation rate [%]; a, b, c are constants; $ep(t)$ is the electricity price [Yen]; $P_L(t)$ is the demand [kW] at time t; $\Delta P_L(t)$ is the response amount [kW] at time t; and $P_{LRTP}(t)$ is the demand [kW] at time t after RTP.

By using piecewise linear function approximation, the variation rate can be expressed as [52]

$$ep(t) = dPL_{X0} + \sum_{P=1}^{k} x_p(t) \tag{25}$$

$$lvr(t) = dPL_{y0} + \sum_{p=1}^{k} \frac{dPL_{y_p} - dPL_{y_{p-1}}}{dPL_{x_p} - dPL_{x_{p-1}}} x_p(t) \tag{26}$$

$$0 \le x_p(t) \le dPL_{x_p} - dPL_{x_{p-1}}, \quad (1 \le p \le k) \tag{27}$$

$$\begin{cases} x_p \ge \left(dPL_{x_p} - dPL_{x_{p-1}}\right) u_p \\ x_{p+1} \le \left(dPL_{x_{p+1}} - dPL_{x_p}\right) u_p \end{cases} \quad (1 \le p \le k) \tag{28}$$

where k is the number of division, x_p is decision variables, and u_p is 0–1 variables.

4. Objective Function

The objective function is used to minimize the system cost in case of no seawater electrolysis plant (scenarios 1 and 2), as shown in Equation (29), and to maximize the profit of the system which comes from chemical products in case of using electrolysis plant (scenarios 3 and 4), as shown in Equation (30),

$$min : \sum_{i=1}^{I} n_i Cost_i \tag{29}$$

$$I = \{PV.WG, BESS, FC.Tank, Comp\}$$

$$max : R_c - \sum_{i=1}^{I} n_i Cost_i \tag{30}$$

where i is the index of equipments, I is the set of equipments, n_i is the number of installed components, $Cost_i$ is the equipment cost [Yen] of index i, and R_c is the revenue of chemical products.

4.1. MILP

Mixed-integer linear programming (MILP) is a numerical advanced optimization tool and practicable program in which some or all of the parameters are limited to integers, and the objective function and constraints are all linear. MILP is successful in problems with a blend of integer, binary, and real-valued variables. Due to its modeling ability, its commercial availability of robust solvers and decision-making for the uncertainty operation, MILP techniques have been used in different applications like modeling and control of hybrid systems, although its computational complexity. MILP is commonly utilized using a branch-and-bound algorithm [53,54].

4.2. System Constraints

Batteries charging and discharging constraints:

$$u_c(t) + u_d(t) \leq 1 \tag{31}$$

The state of charge (SOC) constraints:

$$0.2 n_B cap_B \leq \sum_{t=1}^{j} \left(\eta_c P_c(t) - \frac{1}{\eta_d} P_d(t) \right) + SOC_{ini} \tag{32}$$

$$\sum_{t=1}^{j} \left(\eta_c P_c(t) - \frac{1}{\eta_d} P_d(t) \right) + SOC_{ini} \leq 0.8 n_B cap_B \tag{33}$$

Maximum limit constraint of each component:

$$P_c \leq n_B P_c^{max} \tag{34}$$

$$P_d \leq n_B P_d^{max} \tag{35}$$

$$P_{FC} \leq n_{FC} P_{FC}^{max} \tag{36}$$

Hydrogen Filling Rate (HFR) constraints:

$$0.05 n_T cap_T \leq \sum_{t=1}^{j} \left(f P_{El}(t) - \frac{1}{g} P_{FC}(t) \right) + HFR_{ini} \tag{37}$$

$$\sum_{t=1}^{j} \left(f P_{El}(t) - \frac{1}{g} P_{FC}(t) \right) + HFR_{ini} \leq 0.95 n_T cap_T \tag{38}$$

Processing flow rate limits of hydrogen tank and compressor:

$$f P_{El}(t) \leq n_T Q_{H2}^{max} \tag{39}$$

$$f P_{El}(t) * 2.2 * \frac{ln\,(PR_F/0.1)}{ln\,(20/0.1)} \leq n_{Comp} P_{Comp} \tag{40}$$

Power balance limit:

$$n_{PV} P_{PV}(t) + n_{WG} P_{WG}(t) + n_{FC} P_{FC}(t) + n_B\,(P_d(t) - P_C(t)) - P_{El}(t) - P_{Comp}(t) - P_{sur}(t) = P_{LM}(t) \tag{41}$$

Variation constraint of the load power:

$$\sum_{t=1}^{NT} P_L(t) = \sum_{t=1}^{NT} P_{Lm}(t) \tag{42}$$

Rate of increase constraint for electricity prices:

$$ep(t) - ep(t-1) \leq ep_{diff}^{max} \tag{43}$$

where t is the time; u_c is charging state and u_d is discharging state; and n_{PV}, n_{WG}, n_B, n_{FC}, n_T, and n_{Comp} are the number of each component. P_{PV}, P_{WG}, P_c, P_d, P_{FC}, P_{El}, and P_{comp} are the generated and consumed power of each system components; SOC_{ini} is the initial state of charge of BESS; HFR_{ini} is the initial hydrogen flow; $Q_{H_2}^{max}$ is the maximum flow rate; NT is the final step; and ep_{diff}^{max} is the maximum price increase.

5. Simulation

The objective function of this work is optimal generating units sizing achievement to satisfy electric load demand with minimum cost from 100% renewable sources. Several sizing scenarios for the system to meet consumers' electric demand are considered with different combination of generating and energy storage units like PV, WG, BESS, and FC with electrolysis plants. Table 1 shows the available capacity of system components per each unit. Figures 3–5 show the available amount of PV, WG power, and the required load during all-day hours of five days for a hybrid microgrid system in a small Japanese island. The considered four scenarios will be discussed in the following paragraphs. The simulation is done by using MILP optimization algorithm in MATLAB® software on Intel(R) Core(TM) i5-2450M CPU @ 2.50GHz. The Elapsed time for the four scenarios are recorded as 3453.66, 3620.45, 196.69, and 1426.35 s, respectively.

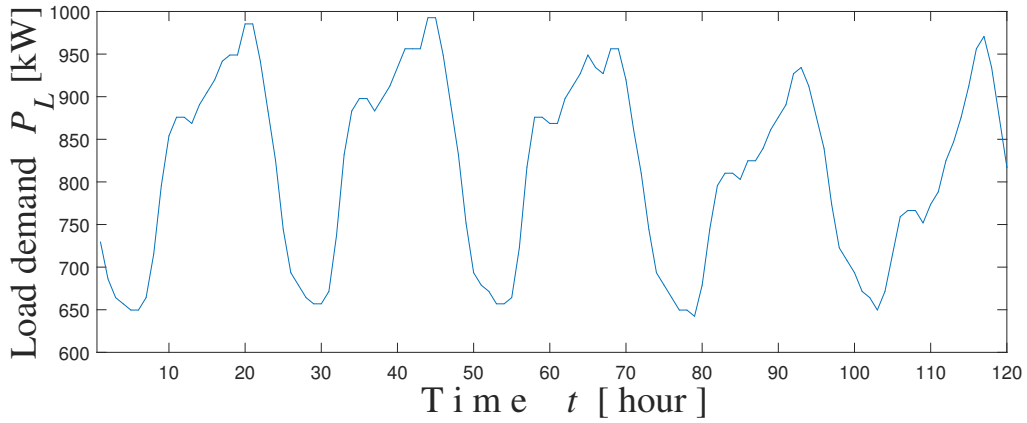

Figure 3. Hourly electrical energy demand.

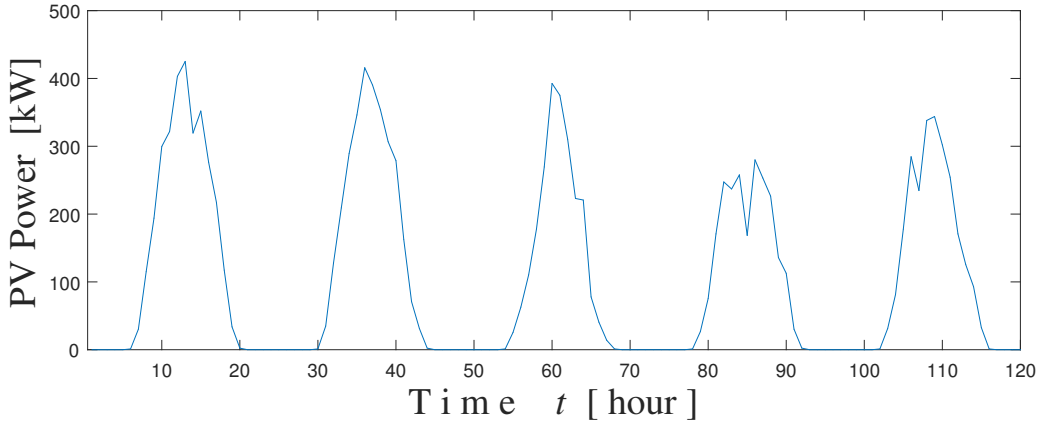

Figure 4. Photovoltaic (PV) power distribution over five days.

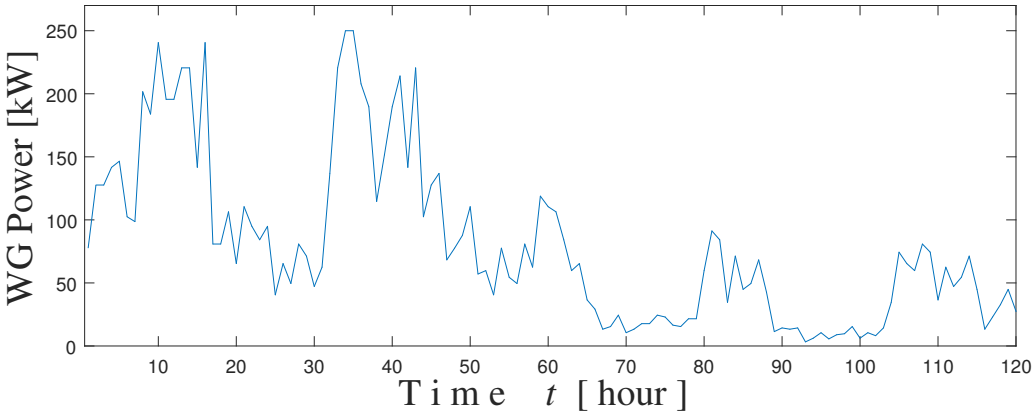

Figure 5. Wind generation power distribution over five days.

Table 1. Available capacity of each of system components.

Item	Capacity/Unit
PV	0.5 MW
WEG	0.25 MW
FC	0.25 MW
Battery	1.2 MWh
Inverter	0.2 MW
Load	1 MW

5.1. Scenario 1

This is the basic power system configuration: it consists of PV and WG as generating units and BESS as a tool to overcome the unavailability of the generated power in adverse weather conditions. It is taken as the reference scenario for comparison with the other scenarios. Table 2 shows the optimal size of PV, wind turbine, and BESS for this scenario that is obtained using MILP solver. Figure 6a presents the generation–load mismatch without BESS, and the generation–load balance taking into consideration BESS is presented in Figure 6b,c showing the SOC of the BESS.

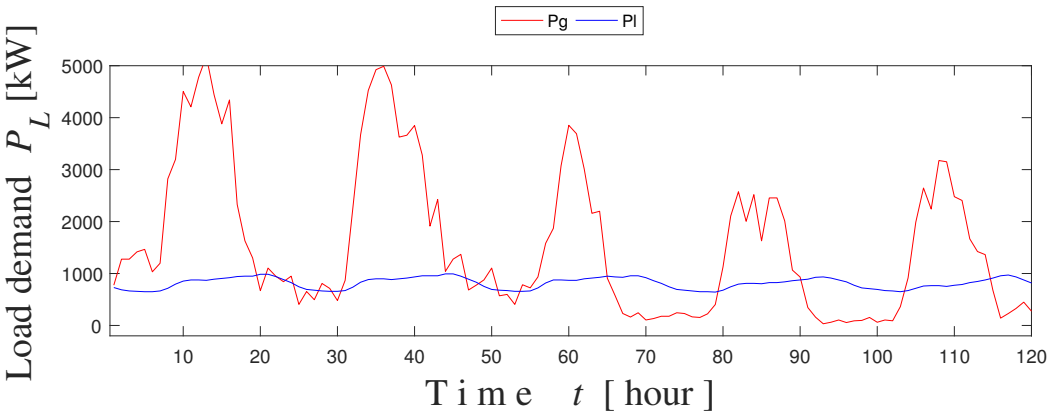

(**a**) Load–generation mismatch.

Figure 6. *Cont.*

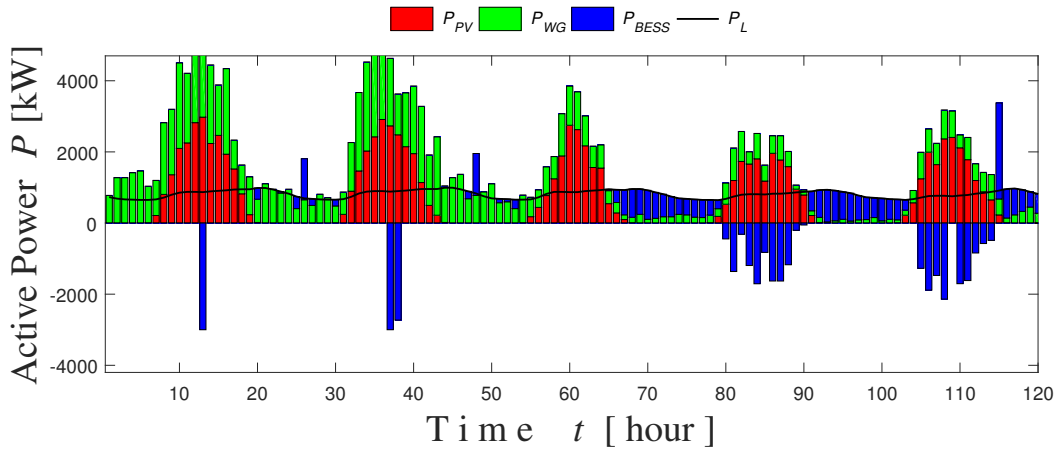

(**b**) Load–generation balance.

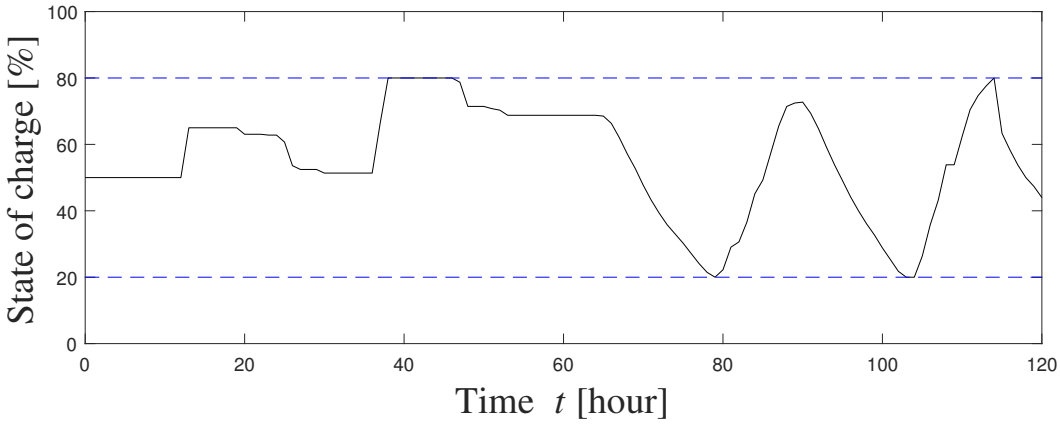

(**c**) State of charge (SOC) of the battery energy storage system (BESS).

Figure 6. scenario 1 results.

Table 2. Scenario 1 results.

	Optimized No. of Units
PV	7
WG	10
BESS	15
Total no of units	32
Cost (millions of Yens)	13.944

5.2. Scenario 2

This scenario is a modified case of scenario (1) by applying RTP demand response to control the load profile according to dynamic changes in prices. Figure 7b shows generation–load mismatch without BESS, whereas Figure 7a presents the generation–load balance with utilizing BESS. The modified load demand after RTP application is expressed as P_{LRTP}. Figure 7c illustrates BESS's SOC, and Figure 7d shows the electricity price [Yen/KWh] obtained by RTP control scheme. The obtained optimal sizes of PV, WG, and BESS are presented in Table 3.

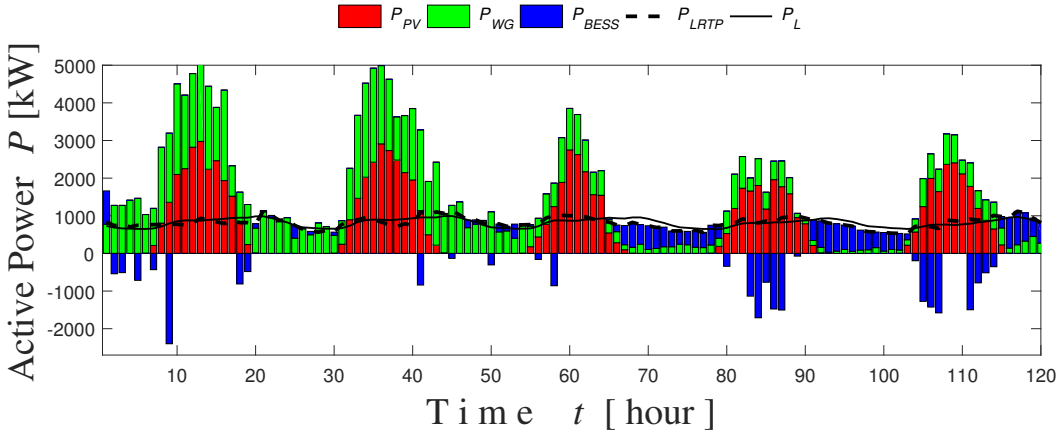

(**a**) Load–generation balance.

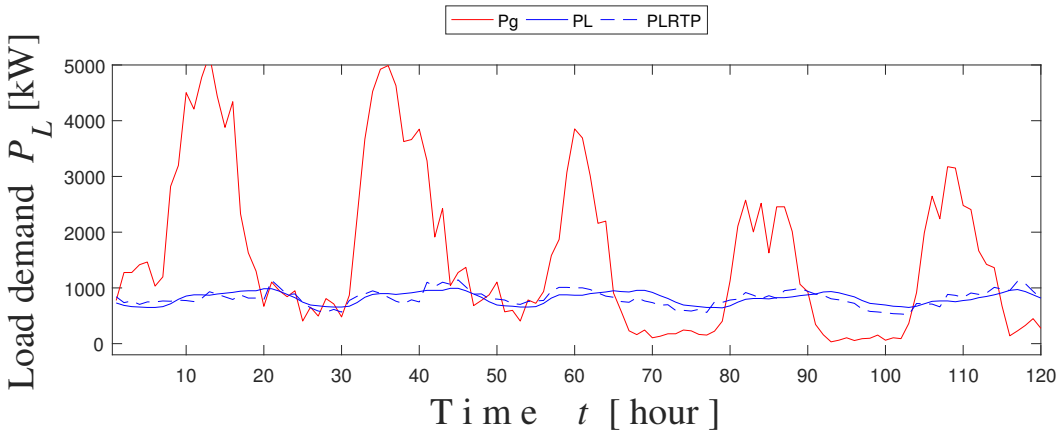

(**b**) Load–generation mismatch.

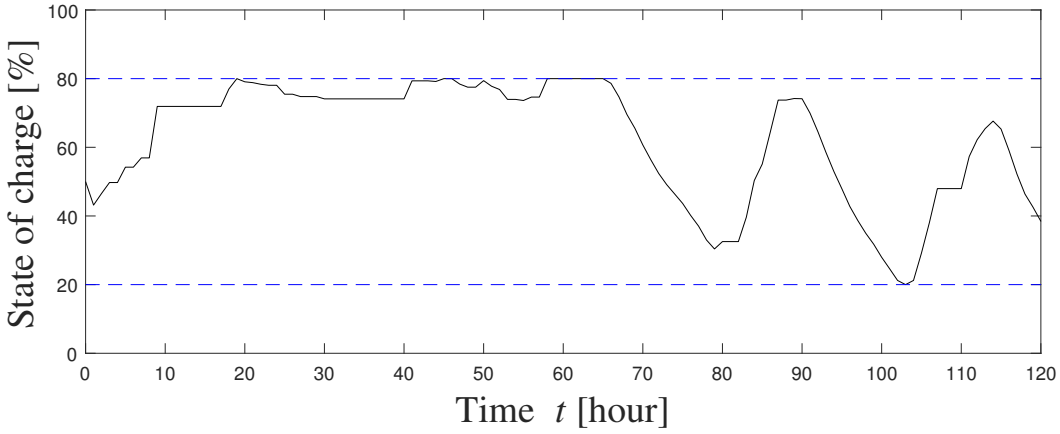

(**c**) SOC of the BESS.

Figure 7. *Cont.*

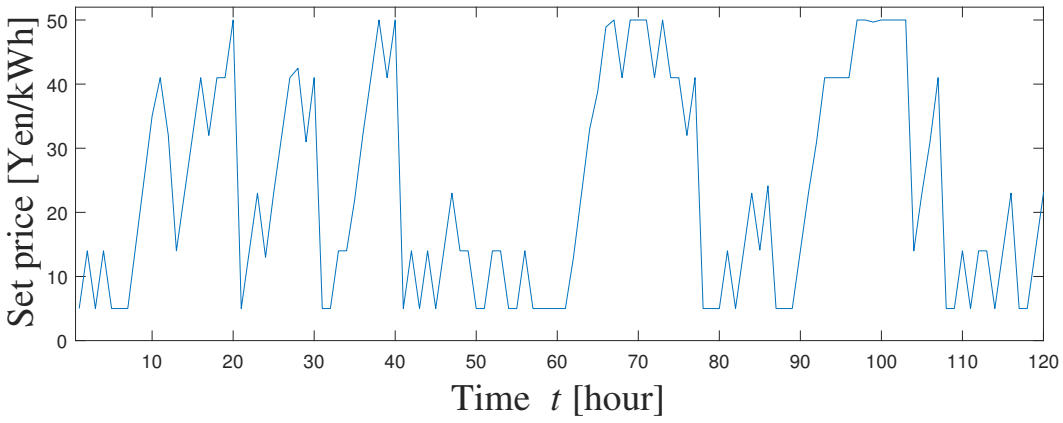

(**d**) Electricity price.

Figure 7. Scenario 2 results.

Table 3. Scenario 2 results.

	Optimized No. of Units
PV	7
WG	10
BESS	12
Total no of units	29
Cost (millions of Yens)	12.6111

5.3. Scenario 3

In this case, FC with the electrolysis plant are introduced. The cost will be logically increased due to FC, compressor, hydrogen tank, and seawater electrolyzes installation. The deciding issue is whether the amount of revenue from marketing chemical products of the electrolyzing process will satisfy and pay back the overall cost or not. The associated optimal sizes of PV, WG, FC, hydrogen tank, and BESS using MILP are shown in Table 4. Table 5 shows the outputs of the electrolysis plant. Figure 8a presents generation–load demand mismatch without FC, whereas Figure 8b shows the generation–load balance with FC and seawater electrolysis plant. Moreover, the hydrogen filling rate is shown in Figure 8c, whereas Figure 8d shows the sodium hypochlorite quantity per ton.

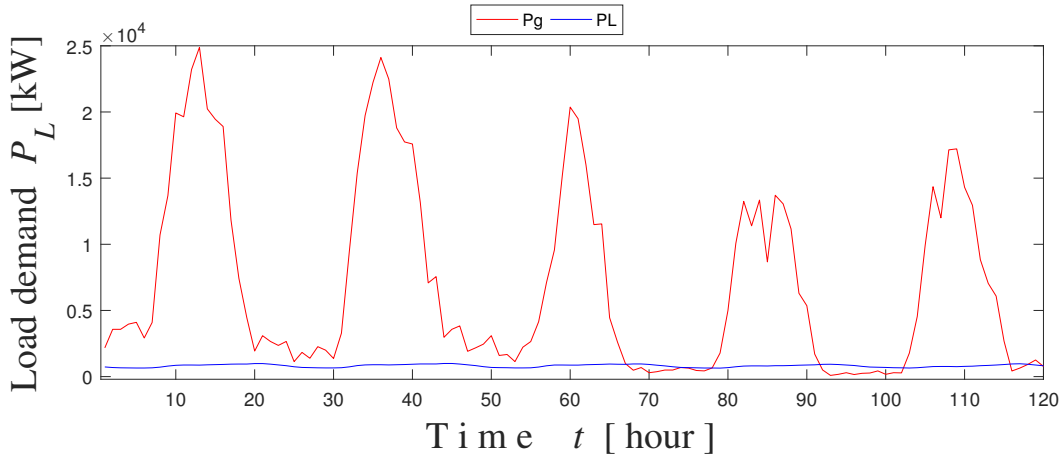

(**a**) Load–generation mismatch.

Figure 8. *Cont.*

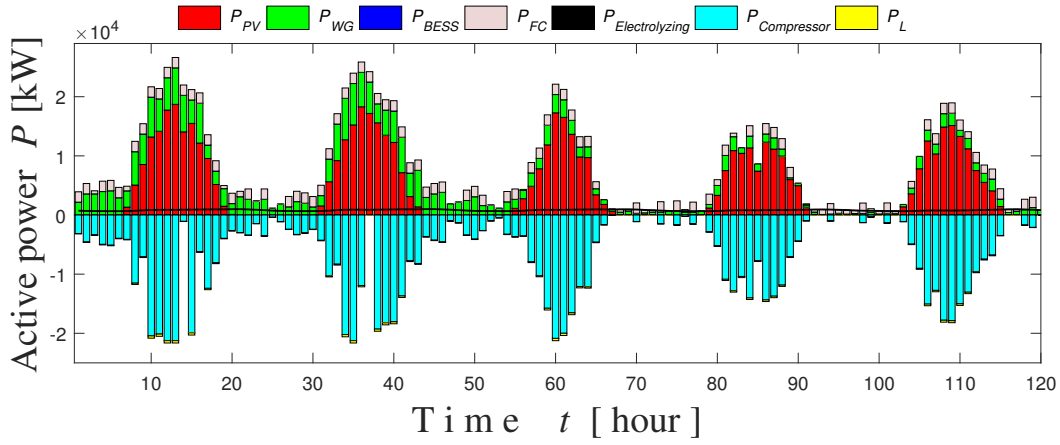

(**b**) Load–generation balance.

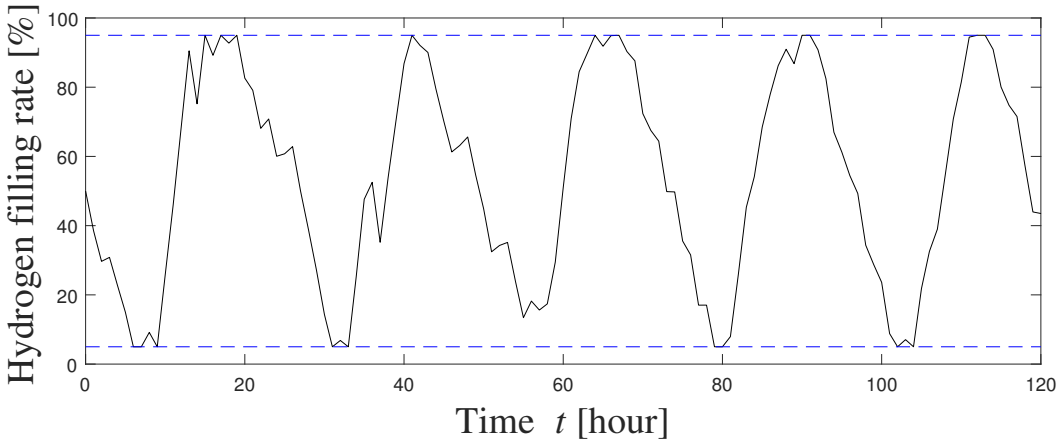

(**c**) Hydrogen filling rate.

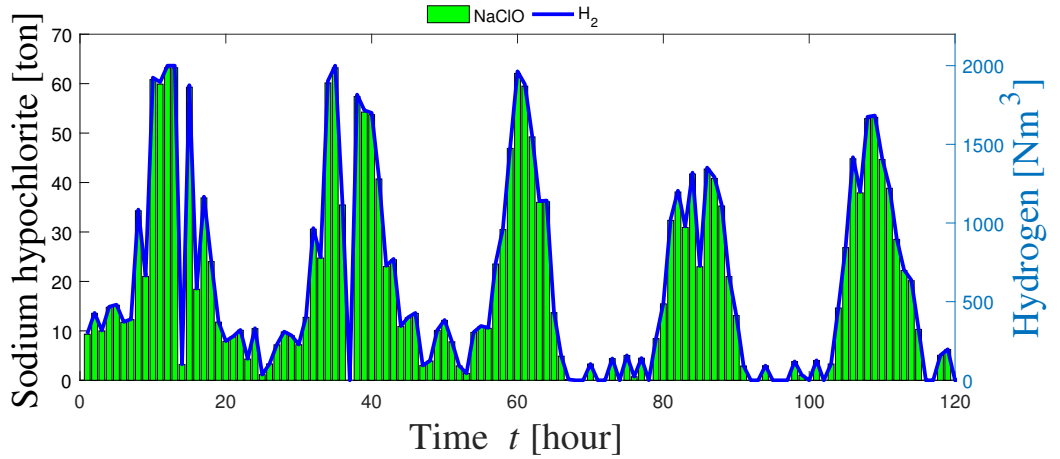

(**d**) Seawater electrolysis plant outputs.

Figure 8. Scenario 3 results.

Table 4. Scenario 3 results.

	Optimized No. of Units
PV	44
WG	28
BESS	0
FC	7
Hydrogen tanks	2
Total no of units	81
Cost (millions of Yens)	49.774
Revenue of chemical products (millions of Yens)	178.054

Table 5. Price and amount of electrolysis plant outputs.

Product	**Price**	**Quantity**
H_2	21.6 (Yen/Nm^3)	0.0941 (Nm^3/kwh)
NaClO	40 (Yen/kg)	312 (g/kwh)

5.4. Scenario 4

In this case, the system is the same as the previous scenario, but with the inclusion of RTP demand response programs. Table 6 shows the optimal sizes of PV, WG, BESS, FC, hydrogen tank, and compressor obtained in this scenario. Figure 9a shows generation–load mismatch without FC and electrolysis plant. Figure 9b presents generation–load balance. Moreover, the hydrogen filling rate, the set price [Yen/Kwh] with RTP application, and the sodium hypochlorite quantity per ton in this scenario are represented in Figure 9c–e, respectively.

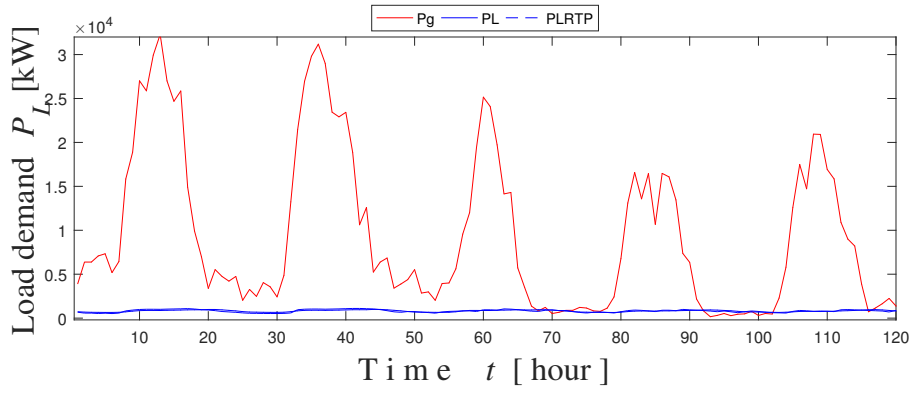

(**a**) Load–generation mismatch.

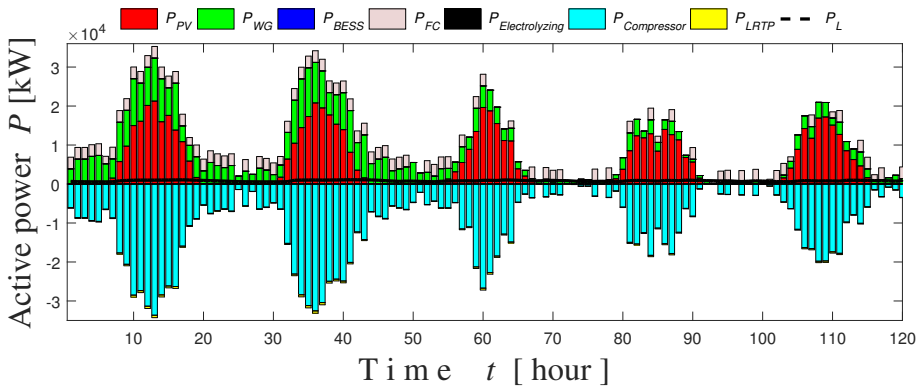

(**b**) Load–generation balance.

Figure 9. *Cont.*

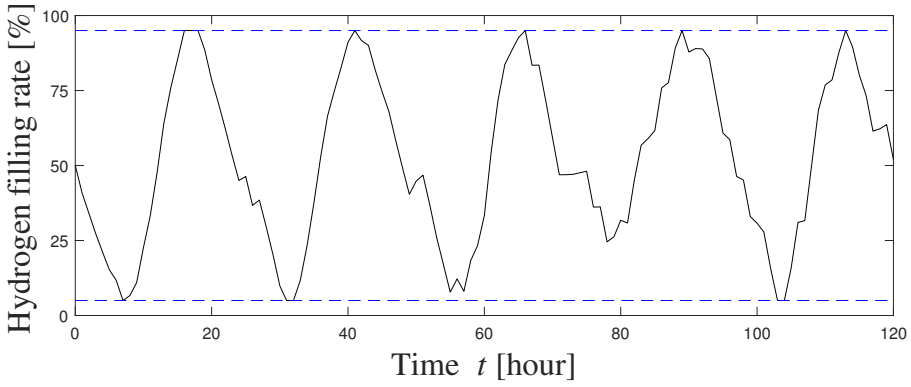

(**c**) Hydrogen filling rate.

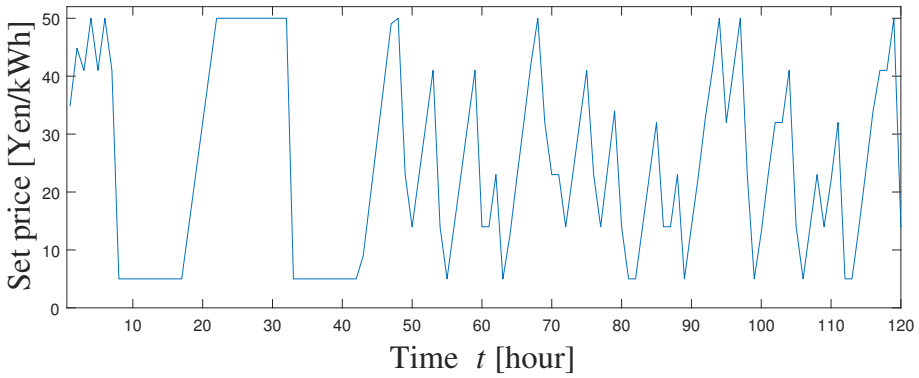

(**d**) Electricity price.

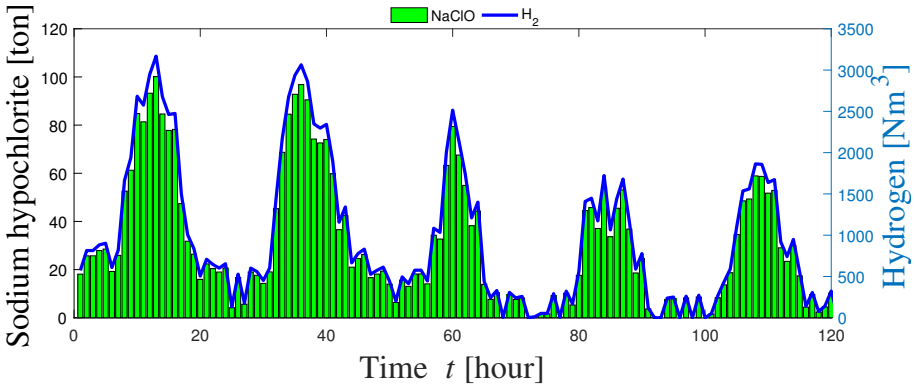

(**e**) Seawater electrolysis plant outputs.

Figure 9. Scenario 4 results.

Table 6. Scenario 4 results.

	Optimized No. of Units
PV	50
WG	50
BESS	0
FC	12
Hydrogen tanks	4
Total no of units	116
Cost (millions of Yens)	75.2386
Revenue of chemical product (millions of Yens)	779.0436

6. Discussion

In all scenarios, the load is met with optimal sizing using MILP techniques. FC combined with seawater electrolysis implementation and RTP application aid in increasing the revenue and achieving the most economical gain of the system. Thus, the simulation results for the four scenarios confirm the following features.

1. Scenario (1) is considered as the basic and reference case with the implementation of PV, WG, and BESS to meet the load demand. The associated simulation results show the ability to meet the load demand with a total cost of 13.944 million yen.
2. It is found that the proposed control scheme in scenario (2) is able to meet the modified load demand of RTP with a decreased number of BESS units compared to scenario (1). This reduction of BESS is ~20% as compared to scenario (1) due to load factor increase of scenario (2) after applying RTP. This achievement in scenario (2) leads to 1.3 million yen reduction in the total system cost compared to scenario (1).
3. Using seawater electrolysis plants reduces the number of BESS to zero, but the number of generating units is significantly increased as seen from scenario (1) and (3) results. The total number of scenario (3) units is raised by 1.5 times the units of scenario (1) and the revenue from chemical products reached 178.054 million yen.
4. The objective function of profit maximization is entirely satisfied by applying RTP demand response programs to scenario (3), as shown from the scenario (4) results in Table (6), which recorded the maximum value of revenue minus the total cost. In this scenario, the largest number of units (116 units) is implemented so as to have sufficient power to produce more hydrogen and chemicals. This action leads to a total system cost of 75.2386 million yen. However, a significant revenue increase compared to scenario (3) is achieved.
5. By considering hydrogen and chemical products, the accumulated revenue of selling these products will cover the total system cost within the project life cycle. For twenty-year project lifetime, it is found using detailed cost calculation with revenue comparison that scenario 4 will pay back and cover the project expenses after 1.068 years, while scenario 3 will take 5.0137 years to reach this target due to the different number of production units.

All scenarios tried to satisfy optimal sizing and minimum cost, but using RTP demand response programs with seawater electrolysis plant makes the system more economically profitable.

7. Conclusions

This paper discusses the optimal sizing of a renewable microgrid in a remote Japanese island, with the introduction of demand response and seawater electrolysis facilities. The mixed-integer linear programming technique is utilized for sizing with maximization of system revenues compared to the total cost as an objective function. Four scenarios of sizing are presented to meet the load requirements: the first scenario is considered as the basic case study with the implementation of PV, WG, and BESS to meet the load demand. The RTP demand program is considered in scenario (2). The seawater electrolysis plant is applied in scenario (3) without using demand response programs, whereas the proposed RTP is applied in scenario (4) with the implementation of seawater electrolysis plant.

The investment in power system sector is introduced through the understanding of electrolyzers usage in producing usable chemical substances (NaClO). The idea of investment in power systems assists economic development through revenue generation, job opportunities creation, and new industries establishment. The proposed system also demonstrates the benefits of using seawater electrolysis plant for hydrogen production to keep fuel cell usage and create revenues from selling produced chemical substances obtained during the electrolyzing process. Simulation results confirm the ability of sea water electrolyzers inclusion to pay back the total project cost within 5.0137 years. Moreover, demand response implementation with chemical production will help in covering all the

project expenses within only 1.068 years. Applying different types of demand response (incentive-based and price-based) approaches with a detailed study of their effect on the microgrid performance and a complete analysis of their economic feasibility study are the planned future work.

Author Contributions: Conceptualization, M.M.G. and T.S.; methodology, M.M.G. and T.S.; validation, M.M.G., H.O.R.H. and T.S.; formal analysis and investigation, M.M.G., M.S. and T.S.; writing—original draft preparation, M.M.G. and T.S.; data curation, M.M.G., A.N. and T.S.; writing—review and editing, M.M.G.. H.T., A.M.H. and T.S.; supervision and project administration, T.S. All authors have read and agreed to the published version of the manuscript.

Funding: This research received no external funding.

Conflicts of Interest: The authors declare no conflicts of interest.

Abbreviations

The following abbreviations and symbols are used in this manuscript.

A	Swept Area of the turbine (m^2)
BESS	Battery Energy Storage System
Co_2	Carbon Dioxide
CPP	Critical Peak Pricing
CAP	Capacity Market Program
C_p	Turbine Power Coefficient
$Cost_{comp}$	The Compressor Cost
$Cost_{tank}$	Tank Cost
DR	Demand Response
DLC	Direct Load Control
EDRP	Emergency Demand Response Program
ep(t)	electricity price [Yen]
DF_{PV}	PV derating factor (%)
E_t	Total global irradiance incident on the PV array (kW/m^2)
$E_{T,STC}$	Solar Irradiation incident at STC (1 kW/m^2)
FC	Fuel cell
GHG	Green House Gases
IBP	Incentive Based Program
IL	interruptible Load
k	no of division
lvr	the variation rate
MILP	Mixed Integer Linear Programming
M_{comb}	mass flow
MCFC	Molten Carbonate Fuel Cell
NaClO	Sodium Hypochlorite
n_{cell}	no of cells linked in series
N	Storage Time
P_{H_2}	Partial Voltage of Hydrogen
P_{O_2}	Partial Voltage of Oxygen
P_{H_2o}	Partial Voltage of Water
P_{FC}	Power Output of Fuell Cell
PV	Photo voltaic
PEMFC	Polymer electrolyte membrane Fuel Cell
P_{Pv}	Output Power of PV
$P_{Pv,rated}$	Rated Capacity of the PV array at STC
P_w	Power Output of The Turbine
P_{comp}	Power of Compressor
PR_f	final outlet pressure
P_L	Load Demand
$P_{LRTP}(t)$	the Load Demand at time t after RTP

Q(t)	current capacity of battery
Q_n	nominal limit of battery
Q_{H_2}	Hydrogen flow rate
RTP	Real Time Pricing
R	Universal gas constant
R_c	Revenue of chemical products
SOFC	Solid Oxide Fuel Cell
SoC	State of Charge
TBP	Time Based Program
ToU	Time of Use
T	Temperature
T_{cell}	PV cell Temperature at the current time step (°C)
$T_{cell,STC}$	PV cell Temperature at STC (25 °C)
u_p	0–1 variables
V_{FC}	Output Voltage of Fuel Cell
V_{act}	Activation Voltage
V_{con}	Concentration Losses
V_{ohm}	Ohmic Losses
WG	Wind Generator
x_p	decision variables
α_{temp}	Temperature Coefficient
$\Delta PL(t)$	response amount at time t
ρ_{air}	The air density (kg/m^3)

References

1. Amagai, K.; Takarada, T.; Funatsu, M.; Nezu, K. Development of low-CO_2-emission vehicles and utilization of local renewable energy for the vitalization of rural areas in japan. *IATSS Res.* **2014**, *37*, 81–88. [CrossRef]
2. Deng, X.; Lv, T. Power system planning with increasing variable renewable energy: A review of optimization models. *J. Clean. Prod.* **2020**, *10*, 118962. [CrossRef]
3. Dong, Y.; Shimada, K. Evolution from the renewable portfolio standards to feed-in tariff for the deployment of renewable energy in Japan. *Renew. Energy* **2017**, *107*, 590–596. [CrossRef]
4. Pineda, S.; Bock, A. Renewable-based generation expansion under a green certificate market. *Renew. Energy* **2016**, *91*, 53–63. [CrossRef]
5. Esteban, M.; Zhang, Q.; Utama, A. Estimation of the energy storage requirement of a future 100% renewable energy system in Japan. *Energy Policy* **2012**, *47*, 22–31. [CrossRef]
6. Yao, S.; Zhang, S.; Zhang, X. Renewable energy, carbon emission and economic growth: A revised environmental Kuznets Curve perspective. *J. Clean. Prod.* **2019**, *235*, 1338–1352. [CrossRef]
7. Esteban, M.; Portugal-Pereira, J. Post-disaster resilience of a 100 % renewable energy system in Japan. *Energy* **2014**, *68*, 756–764. [CrossRef]
8. Komiyama, R.; Otsuki, T.; Fujii, Y. Energy modeling and analysis for optimal grid integration of large-scale variable renewables using hydrogen storage in Japan. *Energy* **2015**, *81*, 537–555. [CrossRef]
9. Adewuyi, O.B.; Kiptoo, M.K.; Afolayan, A.F.; Amara, T.; Alawode, O.I.; Senjyu, T. Challenges and prospects of Nigeria's sustainable energy transition with lessons from other countries' experiences. *Energy Rep.* **2020**, *6*, 993–1009. [CrossRef]
10. Liu, Y.; Guan, X.; Li, J.; Sun, D.; Ohtsuki, T.; Hassan, M.M.; Alelaiwi, A. Evaluating smart grid renewable energy accommodation capability with uncertain generation using deep reinforcement learning. *Future Gener. Comput. Syst.* **2020**, *110*, 647–657. [CrossRef]
11. Modak, N.M.; Ghosh, D.K.; Panda, S.; Sana, S.S. Managing green house gas emission cost and pricing policies in a two-echelon supply chain. *CIRP J. Manuf. Sci. Technol.* **2018**, *20*, 1–11. [CrossRef]
12. Liao, J.-T.; Chuang, Y.-S.; Yang, H.-T.; Tsai, M.-S. BESS-Sizing Optimization for Solar PV System Integration in Distribution Grid. *IFAC-PapersOnLine* **2018**, *51*, 85–90. [CrossRef]

13. Masrur, H.; Howlader, H.O.R.; Lotfy, M.E.; Khan, K.R.; Guerrero, J.M.; Senjyu, T. Analysis of Techno-Economic-Environmental Suitability of an Isolated Microgrid System Located in a Remote Island of Bangladesh. *Sustainability* **2020**, *12*, 2880. [CrossRef]
14. Kerdphol, T.; Fuji, K.; Mitani, Y.; Watanabe, M.; Qudaih, Y. Optimization of a battery energy storage system using particle swarm optimization for stand-alone microgrids. *Int. J. Electr. Power Energy Syst.* **2016**, *81*, 32–39. [CrossRef]
15. Adewuyi, O.B.; Shigenobu, R.; Ooya, K.; Senjyu, T.; Howlader, A.M. Static voltage stability improvement with battery energy storage considering optimal control of active and reactive power injection. *Electr. Power Syst. Res.* **2019**, *172*, 303–312. [CrossRef]
16. Wang, Y.; Sun, Z.; Li, X.; Yang, X.; Chen, Z. A comparative study of power allocation strategies used in fuel cell and ultracapacitor hybrid systems. *Energy* **2019**, *189*, 116142. [CrossRef]
17. Siwal, S.S.; Thakur, S.; Zhang, Q.B.; Thakur, V.K. Electrocatalysts for electrooxidation of direct alcohol fuel cell: Chemistry and applications. *Mater. Today Chem.* **2019**, *14*, 100182. [CrossRef]
18. Corgnale, C.; Hardy, B.; Chahine, R.; Zacharia, R.; Cossement, D. Hydrogen storage in a two-liter adsorbent prototype tank for fuel cell driven vehicles. *Appl. Energy* **2019**, *250*, 333–343. [CrossRef]
19. Bizon, N.; Thounthong, P. Fuel economy using the global optimization of the Fuel Cell Hybrid Power Systems. *Energy Convers. Manag.* **2018**, *173*, 665–678. [CrossRef]
20. Nojavan, S.; Zare, K.; Mohammadi-Ivatloo, B. Application of fuel cell and electrolyzer as hydrogen energy storage system in energy management of electricity energy retailer in the presence of the renewable energy sources and plug-in electric vehicles. *Energy Convers. Manag.* **2017**, *136*, 404–417. [CrossRef]
21. Asokan, K.; Subramanian, K. Design of a tank electrolyser for in-situ generation of NaClO. *Proc. World Congr. Eng. Comput. Sci.* **2009**, *1*, 139–142.
22. Kiptoo, M.K.; Lotfy, M.E.; Adewuyi, O.B.; Conteh, A.; Howlader, A.M.; Senjyu, T. Integrated approach for optimal techno-economic planning for high renewable energy-based isolated microgrid considering cost of energy storage and demand response strategies. *Energy Convers. Manag.* **2020**, *215*, 112917. [CrossRef]
23. Cui, B.; Wang, S.; Xue, X. Effects and Performance of a Demand Response Strategy for Active and Passive Building Cold Storage. *Energy Procedia* **2014**, *61* , 564–567. [CrossRef]
24. Parrish, B.; Gross, R.; Heptonstall, P. On demand: Can demand response live up to expectations in managing electricity systems? *Energy Res. Soc. Sci.* **2019**, *51*, 107–118. [CrossRef]
25. Conteh, A.; Lotfy, M.E.; Adewuyi, O.B.; Mandal, P.; Takahashi, H.; Senjyu, T. Demand Response Economic Assessment with the Integration of Renewable Energy for Developing Electricity Markets. *Sustainability* **2020**, *12*, 2653. [CrossRef]
26. Donado, K.; Navarro, L.; Quintero, M.; Christian, G.; Pardo, M. HYRES: A Multi-Objective Optimization Tool for Proper Configuration of Renewable Hybrid Energy Systems. *Energies* **2020**, *13*, 26. [CrossRef]
27. Sorrentino, M.; Adamo, A.; Nappi, G. Optimal sizing of an rSOC-based renewable microgrid. *Energy Procedia* **2019**, *159*, 237–242. [CrossRef]
28. Saiprasad, N.; Kalam, A.; Zayegh, A. Triple Bottom Line Analysis and Optimum Sizing of Renewable Energy Using Improved Hybrid Optimization Employing the Genetic Algorithm: A Case Study from India. *Energies* **2019**, *12*, 349. [CrossRef]
29. Fukuzumi, S.; Lee, Y.-M.; Nam, W. Fuel production from seawater and fuel cells using seawater. *ChemSusChem* **2017**, *10*, 84264–84276. [CrossRef]
30. Srisiriwat, A.; Pirom, W. Feasibility Study of Seawater Electrolysis for Photovoltaic/Fuel Cell Hybrid Power System for the Coastal Areas in Thailand. *IOP Conf. Ser. Mater. Sci. Eng.* **2017**, *241*, 012041. [CrossRef]
31. d'Amore-Domenech, R.;Leo, T.J. Sustainable hydrogen production from offshore marine renewable farms: Techno-energetic insight on seawater electrolysis technologies. *ACS Sustain. Chem. Eng.* **2019**, *7*, 8006–8022. [CrossRef]
32. Badea, G.E.; Caraban, A.; Cret, P.; Corbu, I. Hydrogen generation by electrolysis of seawater. *Ann. Oradea Univ. Fascicle Manag. Technol. Eng.* **2007**, *6*, 244.
33. Aalami, H.A.; Moghaddam, M.P.; Yousefi, G.R. Evaluation of nonlinear models for time-based rates demand response programs. *Int. J. Electr. Power Energy Syst.* **2015**, *65*, 282–290. [CrossRef]
34. Siano, P.; Sarno, D. Assessing the benefits of residential demand response in a real time distribution energy market. *Appl. Energy* **2016**, *161*, 533–551. [CrossRef]

35. Gima, H.; Yoshitake, T. A comparative study of energy security in okinawa prefecture and the state of hawaii. *Evergr. Jt. J. Nov. Carbon Resour. Sci. Green Asia Strateg.* **2016**, *3*, 36–44. [CrossRef]
36. Guaitolini, S.V.M.;. Yahyaoui, I.; Fardin, J.F.; Encarnação, L.F.; Tadeo, F. A review of fuel cell and energy cogeneration technologies. In Proceedings of the 9th International Renewable Energy Congress (IREC), Hammamet, Tunisia, 20–22 March 2018; pp. 1–6.
37. Wang, C.; Nehrir, M.H. Distributed Generation Applications of Fuel Cells. *J. Electr. Power Syst. Res.* **2006**, 244–248. [CrossRef]
38. El Mentaly, L.; Amghar, A.; Sahsah, H. The prediction of the maximum power of PV modules associated with a static converter under different environmental conditions. *Mater. Today Proc.* **2020**, *24*, 125–129. [CrossRef]
39. Jamal, T.; Carter, C.; Schmidt, T.; Shafiullah, G.M.; Calais, M.; Urmee, T. An energy flow simulation tool for incorporating short-term PV forecasting in a diesel-PV-battery off-grid power supply system. *Appl. Energy* **2019**, *254*, 113718. [CrossRef]
40. Zidane, T.E.K.; Adzman, M.R.B.; Tajuddin, M.F.N.; Zali, S.M.; Durusu, A. Optimal configuration of photovoltaic power plant using grey wolf optimizer: A comparative analysis considering CdTe and c-Si PV modules. *Sol. Energy* **2019**, *188*, 247–257. [CrossRef]
41. Komiyama, R.; Fujii, Y. Optimal integration assessment of solar PV in Japan's electric power grid. *Renew. Energy* **2019**, *139*, 1012–1028. [CrossRef]
42. Tripathy, M.; Samal, R.K. A new perspective on wind integrated optimal power flow considering turbine characteristics, wind correlation and generator reactive limits. *Electr. Power Syst. Res.* **2019**, *170*, 101–115. [CrossRef]
43. Shiraz, M.Z.; Dilimulati, A.; Paraschivoiu, M. Wind power potential assessment of roof mounted wind turbines in cities. *Sustain. Cities Soc.* **2020**, *53*, 101905. [CrossRef]
44. Jongerden, M.R.; Haverkort, B.R. Battery Modeling. Tech Report TR-CTIT-08-01. Enschede. 2008. Available online: http://eprints.eemcs.utwente.nl/11645/01/BatteryRep4.pdf (accessed on 9 January 2008).
45. Wen-Yeau, C. The state of charge estimating methods for battery: A review. *ISRN Appl. Math.* **2013**, *2013*, 953792.
46. Abdel-Aal, H.; Zohdy, K.; Abdel-Kareem, M. Hydrogen production using sea water electrolysis. *Open Fuel Cells J.* **2010**, *3*, 1–7.
47. Casson, L.W.; Bess, J.W. On-site sodium hypochlorite generation. *Proc. Water Environ. Fed.* **2006**, *5*, 6335–6352. [CrossRef]
48. Amos, W.A. *Costs of Storing and Transporting Hydrogen*; Technical Report; National Renewable Energy Lab.: Golden, CO, USA, 1999.
49. Jordehi, A.R. Optimisation of demand response in electric power systems, a review. *Renew. Sustain. Energy Rev.* **2019**, *103*, 308–319. [CrossRef]
50. Yan, X.; Ozturk, Y.; Hu, Z.; Song, Y. A review on price-driven residential demand response. *Renew. Sustain. Energy Rev.* **2018**, *96*, 411–419. [CrossRef]
51. Sugimura, M.; Senjyu, T.; Krishna, N.; Mandal, P.; Abdel-Akher, M.; Hemeida, A.M. Sizing and Operation Optimization for Renewable Energy facilities with Demand Response in Micro-grid. In Proceedings of the 2019 20th International Conference on Intelligent System Application to Power Systems (ISAP), New Delhi, India, 10–14 December 2019; pp. 1–5.
52. Padberg, M. Approximating separable nonlinear functions via mixed zero-one programs. *Oper. Res. Lett.* **2000**, *27*, 1–5. [CrossRef]
53. Earl, M.G.; D'Andrea, R. Iterative MILP methods for vehicle-control problems. *IEEE Trans. Robot.* **2005**, *21*, 1158–1167. [CrossRef]
54. Gordon, G.J.; Hong, S.A.; Dudík, M. First-order mixed integer linear programming. In Proceedings of the Twenty-Fifth Conference on Uncertainty in Artificial Intelligence, Montreal, QC, Canada, 18–21 June 2009; pp. 213–222.